

OPTIMISATION OF GATE TIME PARAMETERS FOR DIFFUSE FIELD NONLINEAR ARRAY IMAGING

Benjamin D Robinson¹, Anthony J Croxford, Bruce W Drinkwater
University of Bristol, UK

ABSTRACT

The requirement for a diffuse field in nonlinear imaging is integral to the performance of the technique, if the statistical conditions are not met by either taking a signal early in time or too late in time, the image performance will be degraded. Metrics to define the level of diffusivity such as phase coherence and standard deviation of energy are investigated to determine their suitability to define a diffuse state. These are compared against SNR in a nonlinear image to confirm they accurately determine a suitable gate time. In addition, the effect of gate length on the characterization of a diffuse field is investigated to determine an optimum duration. Together these provide a set of tools to determine the best parameters for nonlinear array imaging.

Keywords: Nonlinear, arrays, fatigue, diffuse, crack tips

1. INTRODUCTION

The use of phased array imaging in NDT has become prevalent in-order to detect and monitor mechanical fatigue. Linear techniques have proved to be successful in imaging large damage, ie from open cracks, but have not proved successful in detecting smaller closed fatigue cracks [1]. The use of nonlinear diffuse imaging has proven to be an effective method for the detection of these crack tips, or closed surfaces [2, 3], proving successful in detecting early stages of fatigue and monitoring crack growth [4].

The nonlinear technique used here relies on energy movement away from the fundamental caused by nonlinear cracks tips and the ability to spatially resolve this using phased arrays. Two transmission modes are required for the method: sequential and parallel. The material is under more stress in the parallel case and therefore a metric of nonlinearity can be derived from a sequential-parallel field subtraction of the energy at the fundamental frequency. The key requirement of this technique is that the energy is diffuse throughout the specimen to ensure the difference can be related to that seen at the focal spot, meaning the relative loss of energy from the focal point diffuses uniformly [2, 4]. Further in time, the field will be more diffuse however the

influence of noise is higher, meaning a low signal-noise-ratio (SNR). Therefore, characterisation of the diffuse field and far field noise is a necessity to automate this nonlinear technique.

2. MATERIALS AND METHODS

The material used for this study was Aluminum (2014T6, $\sigma \approx 6000 \text{ ms}^{-2}$), which was loaded using a three-point cyclic method according to the standards ATSM- E1820 to produce a closed fatigue crack. To interrogate the structure a Verasonics array controller was used with an Imasonic 5MHz 64 element array.

In-order to assess the influence of volume on reaching a diffuse field, and therefore the reliability of the metrics selected the specimen was machined down from a single initial specimen. Figure (1) displays the 3 geometric alterations on the sample.

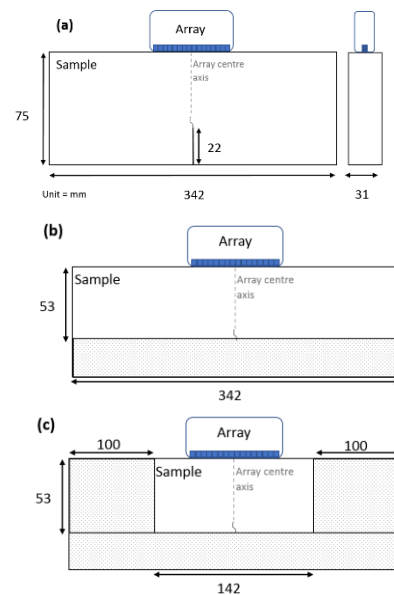


FIGURE 1 - DRAWINGS OF GEOMETRIES FOR SAMPLE SIZES: (A) SAMPLE A - $8.0 \times 10^5 \text{ MM}^3$, (B) SAMPLE B - $5.6 \times 10^5 \text{ MM}^3$ AND (C) SAMPLE C - $2.3 \times 10^5 \text{ MM}^3$

¹ Contact author: benjamin.robinson@bristol.ac.uk

2.1 DIFFUSE FIELD METRICS

The determination of a diffuse field has been of interest throughout multiple fields such as ultrasonics [6], ocean and room acoustics [7,8] seismology and engineering for structural health monitoring [8]. A diffuse field is defined as fields that are globally equi-partitioned [8] and having all normal modes having uncorrelated amplitudes with equal mean squares [4,5,6]. This definition is most appropriate where modes are equally excited and in a finite system. Research into characterisation of diffuse fields in NDT is limited, however investigations on diffuse fields in finite systems and poly-crystals is applicable to NDT [1,4,6].

To characterise a diffuse field, two metrics have been derived and applied to full matrix capture (FMC) phased array imaging: phase coherence and the standard deviation of energy across the array. The phase coherence metric is defined as

$$\alpha(\tau)_{ph} = \frac{\sum_{i=1}^N \int_{-\frac{T}{2}}^{+\frac{T}{2}} (\sum_{j=1}^N f_{i,j}(\tau))^2 d\tau}{\sum_{i=1}^N \sum_{j=1}^N \int_{-\frac{T}{2}}^{+\frac{T}{2}} f_{i,j}(\tau)^2 d\tau} \quad (1)$$

where τ denotes the temporal window, f is the time domain signal, N is the number of elements and i^{th} and j^{th} are the transmitter and receivers respectively.

The standard deviation of energy across the array is defined as

$$\sigma_{en}(\tau) = \frac{1}{N} \sum_{i=1}^N \left[\left(\frac{1}{N} \sum_{j=1}^N (E_{i,j}(\tau) - \bar{E}_i(\tau))^2 \right)^{\frac{1}{2}} \right] \quad (2)$$

where E is the energy of the time-domain signal.

The reliability of these metrics in determining a diffuse field will be the focus of this study.

3. RESULTS AND DISCUSSION

The nonlinear image results from sample size A (the largest volume geometry) for gate time 0.1ms and 0.2ms are displayed in figure 2. The effect of an early gate, where the field is not diffuse, clearly perturbs the SNR of the nonlinear image and will affect the probability of detection. The later gate time of 0.2ms has allowed the energy in the material to become fully diffuse, resulting in a higher SNR across the image. For consistency across images, we define the signal as the maximum nonlinear metric value in the white box. Any value within the red box is considered noise, the position of these regions is set to ensure separability of signal and noise. The mean of this noise is taken, and then the SNR calculated.

A nonlinear experiment was conducted at multiple gate times to measure the effect of this parameter on SNR. It is clear from figure 3 that resolution of the nonlinear feature is highest at 0.3 ms.

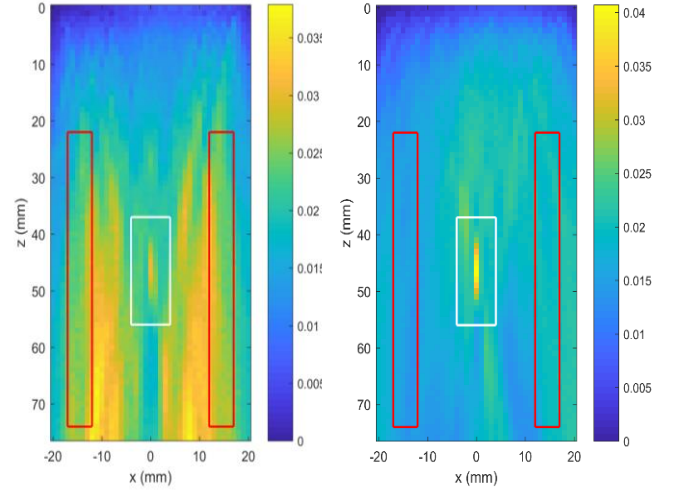


FIGURE 2 - NONLINEAR IMAGES OF SAMPLE A FOR MULTIPLE GATE TIMES: (A) 0.05MS (B) 0.2MS.

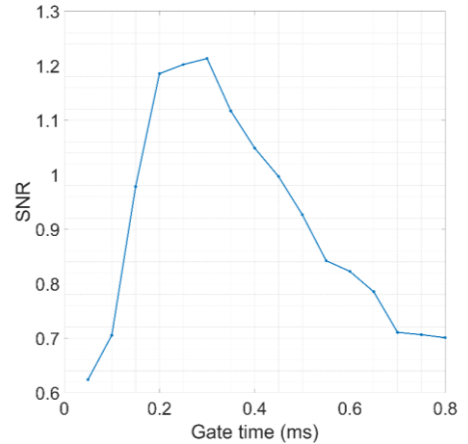


FIGURE 3 - SNR RESULTS FOR SAMPLE A FOR VARIOUS GATE TIMES

The phase coherence metric results for various temporal windows are presented in figure 4. It is important to explore different window lengths as the convergence of this metric around 0.3 ms suggests this metric is reliable in characterising when the field is diffuse. We can also derive that the most appropriate temporal window for this specimen is a $20 \mu\text{s}$ as this length allows for the convergence to be reliably calculated whilst using less data points, reducing computational expense. Using a $50 \mu\text{s}$ window distorts the convergence of this metric and the approximation is too coarse causing the convergence to occur incorrectly later in time.

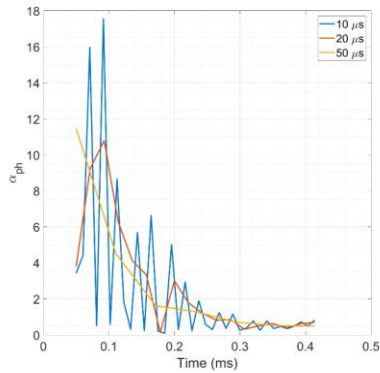


FIGURE 4 - PHASE COHERENCE METRIC RESULTS FOR MULTIPLE TEMPORAL WINDOWS: 10 MS (BLUE), 20 MS(RED) AND 50 MS (YELLOW)

This metric was then applied to all the samples to investigate the effect of sample size on the time to reach a diffuse state. Figure 4 displays the results for these samples using a temporal window of $20 \mu\text{s}$ in all cases. As expected, the lower volume samples have an earlier convergence time as a diffuse field will be reached earlier for smaller samples. This validates the metric to be used across various samples sizes

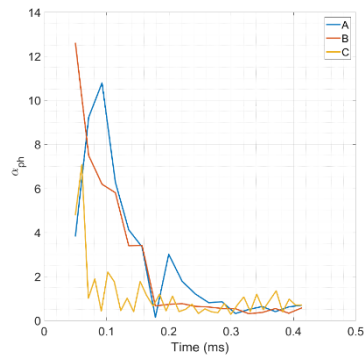


FIGURE 5 – PHASE COHERENCE RESULTS: SAMPLE A (BLUE), SAMPLE B (RED) AND SAMPLE C (YELLOW)

The standard deviation of energy metric for multiple samples sizes is presented in figure 6. This metric is not a function of volume and does not converge at delayed intervals for the different volumes.

4. CONCLUSION

This study concludes that only the phase coherence metric is suitable for determining a diffuse field due to its strong convergence with the highest SNR for various gate times. In addition, this metric has proved effective and robust for multiple geometries. The standard deviation of energy metric shows no convergence, and therefore will not be explored further in this study.

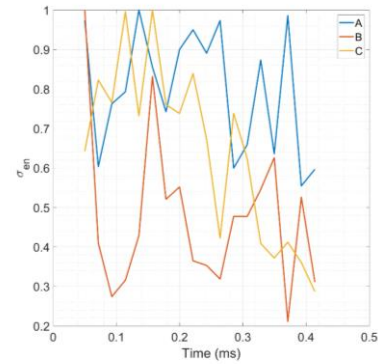


FIGURE 4-RESULTS OF THE STANDARD DEVIATION OF ENERGY METRIC: SAMPLE A (BLUE), SAMPLE B (RED) AND SAMPLE C (YELLOW)

ACKNOWLEDGEMENTS

This work was funded by the EPSRC, Rolls-Royce, EDF, Hitachi and SKF.

REFERENCES

- [1] C. Holmes, B. Drinkwater and P. Wilcox, "Post-processing of the full matrix of ultrasonic transmit–receive array data for non-destructive evaluation," *NDT E International*, vol. 38, p. 701–711, 2005.
- [2] J. N. Potter, A. C. Croxford and P. D. Wilcox, "Nonlinear ultrasonic phased array imaging," *Phys. Rev. Lett.*, p. 113:144301, 2014.
- [3] J. Potter and A. Croxford, "Characterization of nonlinear ultrasonic diffuse energy imaging," *IEEE Transactions on Ultrasonics, Ferroelectrics, and Frequency Control*, pp. 1-1, 2018.
- [4] J. Cheng, J. N. Potter, A. J. Croxford and B. W. Drinkwater, "Monitoring fatigue crackgrowth using nonlinear ultrasonic phased array imaging," *Smart Mater. Struct*, p. 26:055006, 2017.
- [5] P. Nagy, "Fatigue damage assessment by nonlinear ultrasonic materials characterization," *Ultrasonics*, pp. 375-381, 1998.
- [6] R. Weaver, "Diffusivity of ultrasound in polycrystals," *Journal of the Mechanics and Physics of Solids*, p. 38:55–86, 1990.
- [7] P. Roux, K. Sabra and A. Roux, "Ambient noise cross correlation in free space: Theoretical approach," *The Journal of the Acoustical Society of America*, vol. 117, 2005.
- [8] A. Duroux, J. Sabra, J. Ayers and M. Ruzzene, "Extracting guided waves from cross-correlations of elastic diffuse fields: Applications to remote structural health monitoring," *The Journal of the Acoustical Society of America*, pp. 204-215.